MCB
Journals.ASM.org

Stomatin-Like Protein 2 Is Required for *In Vivo* Mitochondrial Respiratory Chain Supercomplex Formation and Optimal Cell Function

Panagiotis Mitsopoulos,[a] Yu-Han Chang,[a] Timothy Wai,[b] Tim König,[b] Stanley D. Dunn,[c] Thomas Langer,[b] Joaquín Madrenas[a]

Microbiome and Disease Tolerance Centre, Department of Microbiology and Immunology, McGill University, Montreal, Quebec, Canada[a]; Institute for Genetics, Cologne Excellence Cluster on Cellular Stress Responses in Aging Associated Diseases, Center for Molecular Medicine, University of Cologne, Cologne, Germany[b]; Department of Biochemistry, University of Western Ontario, London, Ontario, Canada[c]

Stomatin-like protein 2 (SLP-2) is a mainly mitochondrial protein that is widely expressed and is highly conserved across evolution. We have previously shown that SLP-2 binds the mitochondrial lipid cardiolipin and interacts with prohibitin-1 and -2 to form specialized membrane microdomains in the mitochondrial inner membrane, which are associated with optimal mitochondrial respiration. To determine how SLP-2 functions, we performed bioenergetic analysis of primary T cells from T cell-selective *Slp-2* knockout mice under conditions that forced energy production to come almost exclusively from oxidative phosphorylation. These cells had a phenotype characterized by increased uncoupled mitochondrial respiration and decreased mitochondrial membrane potential. Since formation of mitochondrial respiratory chain supercomplexes (RCS) may correlate with more efficient electron transfer during oxidative phosphorylation, we hypothesized that the defect in mitochondrial respiration in SLP-2-deficient T cells was due to deficient RCS formation. We found that in the absence of SLP-2, T cells had decreased levels and activities of complex I-III$_2$ and I-III$_2$-IV$_{1-3}$ RCS but no defects in assembly of individual respiratory complexes. Impaired RCS formation in SLP-2-deficient T cells correlated with significantly delayed T cell proliferation in response to activation under conditions of limiting glycolysis. Altogether, our findings identify SLP-2 as a key regulator of the formation of RCS *in vivo* and show that these supercomplexes are required for optimal cell function.

Stomatin-like protein 2 (SLP-2) is a mainly mitochondrial protein that is widely expressed and is highly conserved across evolution (1–4). We have previously shown that SLP-2 binds the mitochondrial phospholipid cardiolipin and interacts with prohibitin-1 (PHB1) and PHB2, which are proposed to form specialized cardiolipin-enriched microdomains in the mitochondrial inner membrane important for optimal respiratory function (5, 6). Indeed, we showed that deletion of *Slp-2* results in decreased cardiolipin microdomains and increased mitochondrial respiration uncoupled from ATP synthase activity, a defect overcome by an increased reliance on glycolysis (5).

Recently, it has been shown that mitochondrial respiratory complexes are not randomly dispersed throughout the mitochondrial inner membrane but instead have supramolecular interactions allowing them to form respiratory chain supercomplexes (RCS) (7–10). RCS are commonly isolated from mitochondrial membranes with mild detergents, usually digitonin, followed by blue native (BN) polyacrylamide gel electrophoresis (PAGE), and their existence has been confirmed by electron microscopy and single-particle image processing (11, 12). RCS occur mainly among complexes I, III, and IV (NADH-coenzyme Q reductase, ubiquinol-cytochrome *c* reductase, and cytochrome *c* oxidase, respectively) with various stoichiometries, whereas complex V (ATP synthase) can form dimers and oligomers (10, 13) and complex II (succinate-coenzyme Q reductase) is thought to remain fluid (8, 14). Coenzyme Q and cytochrome *c* have also been shown to associate with RCS (15), and recent evidence indicates that there are two distinct pools of coenzyme Q that are dedicated to reducing equivalents from NADH or reduced flavin adenine dinucleotide (16). RCS assemble to facilitate more-efficient electron transfer and to allow the utilization of different electron transport pathways and substrates during oxidative phosphorylation, to stabilize complex I and other complexes, and to limit the production of reactive oxygen species (ROS) generated from electron transport during oxidative phosphorylation (8, 14, 16–19). Altogether, these effects support the importance of RCS for optimal mitochondrial function.

The molecular machinery involved in the formation, maintenance, and regulation of RCS is not well characterized. The defects in RCS assembly/stability observed in some human genetic diseases have provided clues regarding the requirements of RCS formation and maintenance. For example, Barth syndrome, characterized by cardiomyopathy, skeletal myopathy, and neutropenia, is caused by a mutation in the tafazzin gene that impairs cardiolipin remodeling and destabilizes RCS (20), a feature of cardiolipin present in other systems (21, 22). Cardiolipin has been shown to physically bind to complexes I, III, IV, and V (23–25) and to be required for the activities of these complexes (26–28). It has also been suggested that cardiolipin may fill the spaces between com-

Received 14 January 2015 **Returned for modification** 13 February 2015
Accepted 5 March 2015

Accepted manuscript posted online 16 March 2015

Citation Mitsopoulos P, Chang Y-H, Wai T, König T, Dunn SD, Langer T, Madrenas J. 2015. Stomatin-like protein 2 is required for *in vivo* mitochondrial respiratory chain supercomplex formation and optimal cell function. Mol Cell Biol 35:1838–1847. doi:10.1128/MCB.00047-15.

Address correspondence to Joaquín Madrenas, joaquin.madrenas@mcgill.ca.

doi:10.1128/MCB.00047-15

plexes organized into RCS. Thus, cardiolipin is an important factor for proper RCS formation.

Several proteins have also been identified to be important for RCS formation. Two related *Saccharomyces cerevisiae* proteins, Rcf-1 and Rcf-2, and a mammalian homolog, hypoxia-induced gene 2A (HIG2A), are necessary for assembly of mature complex IV and affect complex III-IV RCS formation (29–31). Furthermore, supercomplex assembly factor I (SCAFI) has been shown to act as an RCS chaperone by specifically allowing the assembly of complex III-IV supercomplexes (16, 32). The identification of additional factors required to assemble and maintain RCS is necessary to define the mechanisms governing this process and may be important for the modulation of mitochondrial function.

Given our previous findings that SLP-2 forms cardiolipin-enriched microdomains in the mitochondrial inner membrane and that deletion of *Slp-2* results in decreased levels and activities of certain mitochondrial respiratory chain components and increased uncoupled respiration (5), we sought to examine whether SLP-2 is required for the formation of RCS. Here, we show that the efficiency of mitochondrial respiration in primary T cells lacking SLP-2 expression is impaired when the cell must rely almost exclusively on oxidative phosphorylation for energy production and that this effect is associated with decreased amounts of $(\text{I-III}_2)_{1\text{-}2}$ and $\text{I-III}_2\text{-IV}_{1\text{-}3}$ RCS. Functionally, this defect results in decreased T cell proliferation when glycolysis, but not oxidative phosphorylation, is restricted. These data identify SLP-2 as a key regulator of mitochondrial respiratory function by linking the formation of cardiolipin-enriched microdomains with optimal assembly of RCS and point to a functional role for RCS in T cells *in vivo*.

MATERIALS AND METHODS

Mice. T cell-specific *Slp-2* knockout mice in the C57BL/6N Tac background were generated as described previously (5). Briefly, *Slp-2*$^{lox/wt}$ mice were crossed with CD4-Cre mice (Taconic Farms, Hudson, NY) to generate *Slp-2*$^{lox/lox}$/Cre^{+} (SLP-2 T-K/O) or *Slp-2*$^{lox/lox}$/Cre^{-} (wild-type [WT]) mice. Breeding colonies were derived from the same *Slp-2*$^{lox/lox}$ breeders and kept in parallel. Mice were maintained in the animal facility at McGill University with the approval of the Comparative Medicine and Animal Resources Centre in accordance with Canadian Council on Animal Care guidelines.

MEFs. Primary WT and *Slp-2*$^{-/-}$ mouse embryonic fibroblasts (MEFs) were isolated from embryonic day 13.5 *Slp-2*$^{lox/lox}$ conditional embryos (5) and immortalized with a plasmid expressing simian virus 40 large T antigen (33). Immortalized WT and *Slp-2*$^{-/-}$ MEFs were then generated *in vitro* as previously described (34). *Slp-2*$^{-/-}$ clones were confirmed by PCR and immunoblot analyses.

Cell culture. T cells were isolated from WT and SLP-2 T-K/O mouse spleens by negative selection with the EasySep mouse T cell isolation kit (Stemcell Technologies, Vancouver, Canada). Cells were stimulated with 5 μg/ml anti-CD3ε and 2 μg/ml anti-CD28 plate-bound antibodies (eBioscience, San Diego, CA) and cultured in 25 mM glucose- or galactose-containing medium with or without the addition of 1 nM oligomycin. Glucose- and galactose-containing media were prepared from glucose-free RPMI medium supplemented with 25 mM glucose or galactose, 10% dialyzed fetal bovine serum, 1 mM sodium pyruvate, 2 mM L-glutamine, 0.1% β-mercaptoethanol, and penicillin-streptomycin. Immortalized WT and *Slp-2*$^{-/-}$ MEFs were cultured in glucose-free Dulbecco's modified Eagle's medium plus GlutaMAX (Gibco, Carlsbad, CA) supplemented with 25 mM glucose or galactose, 10% dialyzed fetal calf serum (Gibco), 1 mM sodium pyruvate, and nonessential amino acids. Galactose-containing media contained little or no glucose. For cell growth experiments, WT and *Slp-2*$^{-/-}$ MEFs were seeded at 50,000 cells per plate and harvested every 24 h to assess viable cell numbers by trypan blue exclusion. Cells were incubated at 37°C in a humidified atmosphere of 5% CO_2.

Bioenergetic analysis. The oxygen consumption rate (OCR) and extracellular acidification rate (ECAR) were measured with an XF-24 analyzer (Seahorse Bioscience, North Billerica, MA) as described previously (5). Briefly, following stimulation for 48 h, WT and SLP-2 T-K/O T cells were suspended in Seahorse XF assay medium supplemented with 2 mM L-glutamine, 2 mM sodium pyruvate, and 25 mM glucose or galactose and seeded onto XF24 V7 24-well cell culture plates coated with 50 μg/ml poly-D-lysine at 500,000 cells/well. OCR and ECAR (a measure of lactic acid formed during glycolysis) were measured prior to and following the sequential additions of 10 μM oligomycin, 100 nM rotenone, and 1 μM antimycin A. Basal OCR refers to the respiration rate measured prior to the addition of mitochondrial drugs. Mitochondrial OCR was calculated by subtracting the OCR in the presence of rotenone/antimycin A from the basal OCR. Uncoupled OCR refers to oligomycin-insensitive mitochondrial respiration. The percentage of coupled OCR was calculated relative to the total mitochondrial OCR.

BN gel electrophoresis. BN gel electrophoresis was performed on the basis of the method introduced by Schägger and von Jagow, with some modifications (9, 35–37). Briefly, mitochondria of WT and SLP-2 T-K/O T cells stimulated for 48 h were isolated with a Dounce homogenizer and differential centrifugation as described previously (36). Mitochondria were lysed with digitonin (4 g/g of protein) or *n*-dodecyl β-D-maltoside (1.6 g/g of protein) for 5 min and 20 μg of protein was loaded per lane in Novex 3 to 12% Bis-Tris gels (Life Technologies, Grand Island, NY) and run on ice. Crude mitochondria (100 μg) from WT and *Slp-2*$^{-/-}$ MEFs were solubilized in 6 g/g of digitonin and electrophoresed in 3 to 9% gels. First-dimension gels were either denatured with sodium dodecyl sulfate (SDS)-containing buffer for two-dimensional (2D) BN SDS-PAGE, transferred to polyvinylidene difluoride (PVDF) membranes for immunoblotting, stained with silver (Silver Stain Plus kit; Bio-Rad, Hercules, CA), or assayed for in-gel complex I activity (0.1 M Tris-HCl, 0.14 mM NADH, and 1.0 mg/ml Nitro Blue Tetrazolium with gentle agitation [38]). For 2D BN SDS-PAGE, 1D gel slices were cut in half and high- and low-molecular-weight portions of WT and SLP-2 T-K/O slices were loaded onto the same 2D SDS–10% polyacrylamide gel. 2D gels were either transferred to PVDF membranes for immunoblotting or stained with silver.

Immunoblotting. PVDF membranes containing protein transferred from 1D BN PAGE or 2D BN SDS-PAGE gels were blotted with antibodies against subunits of mouse complex I (NDUFA9, NDUFB6, and NDUFS3), complex II (SDHA), complex III (UQCRC2, core 1), complex IV (MTCO1), and complex V (ATP5A) or total OXPHOS antibody cocktail (Mitosciences, Eugene, OR), anti-PHB1 (Santa Cruz Biotechnology, Santa Cruz, CA), and anti-SLP-2 (Protein Tech Group Inc., Chicago, IL). For phospho-IκB detection, WT or SLP-2 T-K/O T cells were stimulated with mouse T activator Dynabeads (Life Technologies) for the times indicated and then washed with ice-cold phosphate-buffered saline containing 400 μM sodium orthovanadate and resuspended in lysis buffer containing 1% Triton X-100 with phosphatase and protease inhibitors for 30 min on ice as described previously (5). Lysates were separated by 10% SDS-PAGE, transferred to a PVDF membrane, and then immunoblotted with anti-phospho-IκB (Ser32), anti-IκB (Cell Signaling, Danvers, MA), anti-SLP-2, and anti-glyceraldehyde 3-phosphate dehydrogenase (anti-GAPDH; Chemicon International, Temecula, CA) antibodies.

ELISA. WT and SLP-2 T-K/O T cells were stimulated for 24 h in glucose- or galactose-containing medium, and interleukin-2 (IL-2) levels were quantified with the mouse IL-2 enzyme-linked immunosorbent assay (ELISA) Ready-SET-Go! kit (eBioscience).

Flow cytometry. To assess T cell proliferation, WT and SLP-2 T-K/O T cells were loaded with 1 μM carboxyfluorescein diacetate succinimidyl ester (CFSE) and then stimulated (1 μg/ml anti-CD3ε, 2 μg/ml anti-CD28, plate bound) in glucose- or galactose-containing medium with or without oligomycin for 0, 2, 3, 4, and 5 days. To measure CD25 and

CD62L expression, cells were blocked with 10 μg/ml Mouse Fc Block (BD Pharmingen, Franklin Lakes, NJ) and then stained with 2 μg/ml mouse BV421 anti-CD62L (BD Horizon), allophycocyanin (APC)–anti-CD25, and APC eFluor 780–anti-CD3 antibodies (eBioscience). For IL-2 supplementation studies, 50 ng/ml mouse recombinant IL-2 (mrIL-2; eBioscience) was added to the culture medium at the start of the experiment. For intracellular IL-2 determination, T cells were treated with BD GolgiPlug (BD Biosciences) containing brefeldin A at the time of anti-CD3/CD28 stimulation, fixed 24 h later with BD Cytofix/Cytoperm (BD Biosciences), and then stained with APC–anti-IL-2 antibody (eBioscience). Viability was assessed with the Zombie Aqua fixable viability kit (BioLegend, San Diego, CA). To assess mitochondrial membrane potential, stimulated WT and SLP-2 T-K/O T cells were stained in nonquench mode with 20 μM tetramethylrhodamine methyl ester (TMRM) for 1 h with no washing (39). ROS levels were assessed by measuring the fluorescence of cells stained with 5-(and 6)-chloromethyl-2′,7′-dichlorodihydrofluorescein diacetate, acetyl ester (Life Technologies). Cell cycle entry was measured with APC-conjugated anti-Ki67 antibody (BioLegend). For calcium release assay, cells were stained with Fluo-3-AM (4 μg/ml) and Fura Red (10 μg/ml; Invitrogen) for 30 min. Following baseline measurement, ionomycin (2 μg/ml), carbonyl cyanide-*p*-triflouromethoxyphenylhydrazone (FCCP; 50 nM), or EDTA (5 mM) was added and fluorescence was measured for 5 min. Flow cytometry was performed with an LSRFortessa flow cytometer (BD), and data were analyzed with FlowJo software (TreeStar Inc., Ashland, OR).

Quantitative reverse transcriptase PCR. WT and SLP-2 T-K/O T cells were cultured for 4, 12, and 24 h with or without anti-CD3/CD28 antibody stimulation in glucose- or galactose-containing medium. Cellular RNA was isolated with the RNeasy Plus minikit (Qiagen, Mississauga, ON, Canada) and quantified with NanoDrop (Thermo Scientific, Wilmington, DE). cDNA was synthesized from 220.08 ng of total RNA with the Omniscript reverse transcription kit (Qiagen), and transcript levels were quantified on the CFX96 real-time system (Bio-Rad) with iTaq Universal SYBR green Supermix (Bio-Rad). The sequences of the primers used were as follows: IL-2, forward primer 5′-CCTGGAGCAGCTGTTG ATGG-3′ and reverse primer 5′-CAGAACATGCCGCAGAGGTC-3′; RPL19, forward primer 5′-AACTCCCGTCAGCAGATCAG-3′ and reverse primer 5′-CATTGGCAGTACCCTTCCTC-3′; hypoxanthine phosphoribosyltransferase (HPRT), forward primer 5′-AGTCCCAGCGTCG TGATTAG-3′ and reverse primer 5′-CAGAGGGCCACAATGTGATG-3′. Relative IL-2 transcript levels were determined by comparing IL-2 threshold cycle (C_T) values for WT or SLP-2 T-K/O T cells stimulated for 4, 12, and 24 h in glucose- or galactose-containing medium to that for nonstimulated T cells and then normalizing them to RPL19 and HPRT expression.

ATP quantification. WT or SLP-2 T-K/O T cells were stimulated with plate-bound anti-CD3/CD28 antibody for 2 days in complete medium and then incubated for 1 h in glucose- or galactose-containing medium prior to measurement of ATP with the ATP determination kit (Molecular Probes, Eugene, OR) as described previously (5).

RESULTS

SLP-2-deficient T cells have increased uncoupled respiration and decreased mitochondrial membrane potential, both exacerbated under conditions of limiting glycolysis. We have previously generated T cell-specific *Slp-2* knockout (SLP-2 T-K/O) mice and shown that deletion of *Slp-2* in T cells *in vivo* negatively impacts the function of the mitochondrial respiratory chain, resulting in decreased levels of some complex I and II subunits, and decreased activities of complexes I and II+III (5). In addition, using extracellular flux technology to assess cellular respiration, we have shown that when glucose is available, SLP-2-deficient T cells from these mice exhibit increased mitochondrial respiration uncoupled from ATP synthase activity. In these T cells, inefficient mitochondrial respiration was compensated for by an increased reliance on glycolysis to preserve function (5). To test the metabolic function of SLP-2 T-K/O T cells under conditions of almost exclusive reliance upon oxidative phosphorylation, we incubated primary WT and SLP-2 T-K/O T cells in medium containing galactose but lacking glucose, thereby severely limiting the glycolytic rate since this sugar enters the glycolytic pathway at a much lower rate than glucose, as it is a much poorer substrate for hexokinase (40). We found that although the basal cellular and mitochondrial OCRs were unchanged between WT and SLP-2-deficient T cells (Fig. 1A and B), there was a trend toward decreased percentage of mitochondrial respiration coupled to ATP synthase activity in SLP-2-deficient T cells cultured in both glucose- and galactose-containing medium relative to WT T cells (Fig. 1C). Though this did not reach statistical significance, analysis of uncoupled mitochondrial respiration rates revealed a significant increase in this parameter in SLP-2-deficient T cells that was significantly greater when glycolysis was limiting (Fig. 1D). This increase in uncoupled mitochondrial respiration is comparable to the increase observed in hearts of a mouse model of diabetes and obesity (41). We also confirmed that cells were respiring normally by using FCCP as a positive control (data not shown). Although total cellular ATP levels were not changed (Fig. 1E), SLP-2-deficient T cells exhibited a decrease in mitochondrial membrane potential when cultured in galactose-containing medium (Fig. 1F), pointing to impaired function of the mitochondrial respiratory chain. This correlated with an increased reliance of SLP-2 T-K/O T cells on glycolysis when cultured in both glucose- and galactose-containing media, as noted by the significantly greater basal ECARs (Fig. 1G). Finally, SLP-2-deficient T cells exhibited increased levels of ROS (Fig. 1H), a characteristic of mitochondrial respiratory chain impairment. Taken together, these data show an impaired mitochondrial respiratory profile in the absence of SLP-2 that was worsened by experimentally limiting the cellular glycolytic rate.

SLP-2 deficiency results in defective RCS formation in cell lines. The makeup of RCS can vary between tissues and species, but RCS are commonly thought to occur as I-III_2-IV_{1-4} or as I-III_2. In the current study, we have estimated RCS stoichiometries based on previous literature (10, 42, 43) and approximate molecular weights. The previous data showing impaired mitochondrial respiratory function in the absence of SLP-2, and our findings that SLP-2 is important for the formation of cardiolipin-enriched membrane microdomains necessary for optimal mitochondrial respiratory function (5, 6), suggested that there might be impaired RCS formation in the absence of SLP-2. To test this, we first generated *Slp-2* knockout MEFs (*Slp-2*$^{-/-}$ MEFs) *in vitro* and performed BN PAGE of WT and *Slp-2*$^{-/-}$ MEF mitochondrial lysates. Immunoblot analyses following BN PAGE showed a dramatic reduction of respiratory complex I (NDUFA9 and NDUFB6), III (UQCRC2), and IV (MTCO1) subunits in RCS, specifically of (I-III_2)$_{1-2}$, I-III_2-IV_3, I-III_2-IV_2, I-III_2-IV, I-III_2, and III_2-IV arrangements (Fig. 2A). The significant reductions in the levels of RCS correlated with a lower growth rate of *Slp-2*$^{-/-}$ MEFs than that of WT controls when cultured in either glucose- or galactose-containing medium (Fig. 2B). Interestingly, *Slp-2*$^{-/-}$ MEFs failed to proliferate when glycolysis was limiting (Fig. 2B, bottom), consistent with our previous findings that SLP-2-deficient cells had impaired mitochondrial respiratory function. Together, these data showed defective RCS formation in MEFs in the absence of SLP-2, which correlated with decreased cell cycling.

Primary SLP-2-deficient T cells have defective RCS forma-

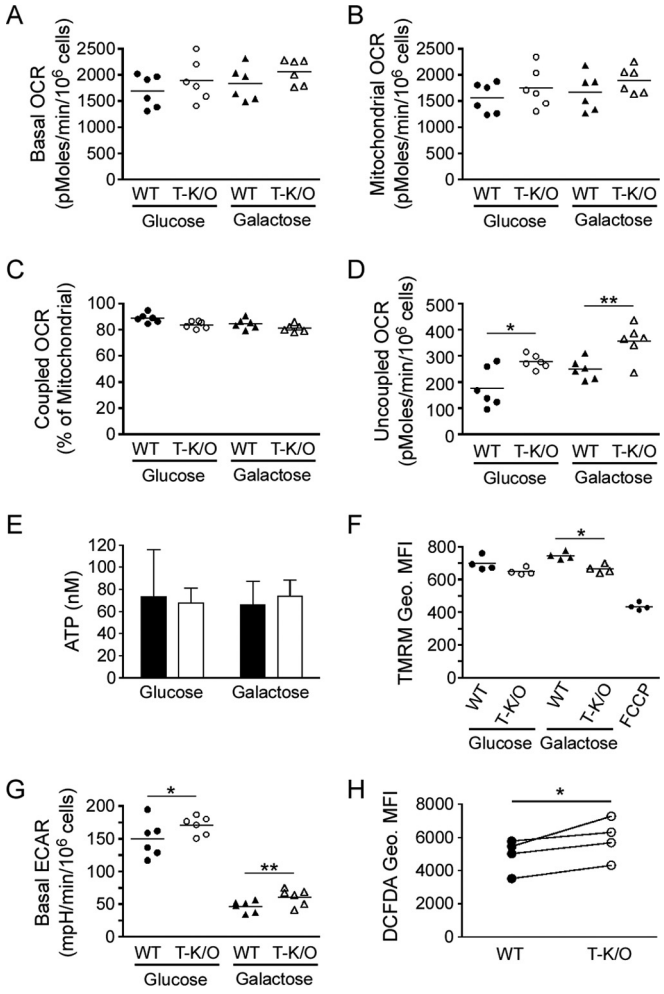

FIG 1 SLP-2-deficient T cells have an impaired mitochondrial respiration profile characterized by increased uncoupled respiration and reliance on glycolysis. T cells from WT (filled symbols or bars) or SLP-2 T-K/O (empty symbols or bars) mice were stimulated for 48 h and then incubated for 1 h in glucose (circles)- or galactose (triangles)-containing medium. Following measurement of the basal OCR (A), the mitochondrial drugs oligomycin, rotenone, and antimycin A were sequentially added to determine the total mitochondrial OCR (B), as well as mitochondrial OCR coupled to (C) or uncoupled from (D) ATP synthase activity. (E) ATP levels were quantified in whole-cell lysates of WT or SLP-2 T-K/O T cells treated as previously indicated ($n = 3$). (F) Mitochondrial membrane potential was measured by flow cytometry in T cells stimulated for 48 h prior to 24 h of incubation under glucose- or galactose-only conditions with TMRM in nonquench mode (FCCP, positive control) ($n = 4$). (G) Basal ECAR, a measure of the glycolytic rate, was measured in T cells concurrently with OCR from panel A. (H) ROS levels were determined in cells treated as described for panel F, by measuring DCFDA geometric mean fluorescence intensity (Geo. MFI) ($n = 4$). (A to D, G) Dot plots depict the mean OCR or ECAR of 10^6 cells of six mice per genotype performed at least in duplicate and analyzed in pairs. (F, H) Each dot represents one mouse, and the mean was calculated for four mice per genotype and analyzed in pairs. *, $P < 0.05$; **, $P < 0.01$ (relative to the WT control in glucose- or galactose-containing medium, as indicated).

tion *in vivo*. Next we assessed RCS formation *in vivo* from mitochondria of primary T cells lacking SLP-2. To do this, we immunoblotted 1D BN PAGE gels of digitonin-solubilized mitochondrial lysates from WT or SLP-2-deficient T cells with antibodies against subunits of respiratory complexes I (NDUFA9 and NDUFS3), III (UQCRC2 and core 1), IV (MTCO1), and V (ATP5A) (Fig. 3A). We found decreased or undetectable amounts of RCS containing complex I and III subunits, specifically of I-III_2-IV_3, I-III_2-IV_2, I-III_2-IV, and I-III_2 arrangements (Fig. 3A). Immunodetection of PHB1 and SLP-2 revealed that these proteins exhibit electrophoretic mobilities conspicuously overlapping those of larger RCS (Fig. 3A). The comigration of PHBs and SLP-2 observed here is in line with previous reports from our group and others that show that SLP-2 associates with PHBs (6, 44).

To further document the decreased complex I association with RCS and its functional significance, we performed a complex I in-gel activity assay on a nondenatured first-dimension gel to visualize enzymatically active complex I (Fig. 3B). Complex I activity, as indicated by the development of purple formazan, was decreased in high-molecular-weight regions corresponding to RCS, including I-III_2-IV_2 and I-III_2 (Fig. 3B).

To corroborate our findings obtained by first-dimension BN PAGE, we cut nondenatured 1D BN PAGE gels of the same aforementioned WT and SLP-2 T-K/O T cell mitochondrial lysates in half and loaded high-molecular-weight (Fig. 3C) and low-molecular-weight (Fig. 3D) portions onto second-dimension SDS-polyacrylamide gels and then immunoblotted them with antibodies directed against subunits of complexes I, II, III, IV, and V. Consistent with the 1D BN PAGE results, we observed lower levels of complex I, III, and IV subunits associated with RCS in mitochondria of SLP-2-deficient T cells than in WT controls, including I-III_2-IV_3, I-III_2-IV_2, I-III_2-IV, and I-III_2 arrangements (Fig. 3C). The migration of MTCO1 with RCS, faintly detectable by 1D BN PAGE analysis (Fig. 3A), can be better visualized by 2D BN SDS-PAGE analysis (Fig. 3C). Complex V has been reported to associate with RCS under certain circumstances (15) but has also been commonly found to associate into dimers and multimers (10, 13). We found that this technique was sufficiently sensitive to show migration of complex V at various regions of high molecular weight that correspond to the migration patterns of RCS, suggesting that these may be multimers of complex V or perhaps associations with certain RCS (Fig. 3C). However, the multimers of complex V were decreased or absent upon *Slp-2* deletion (Fig. 3C). The levels of non-RCS-associated complexes did not appear different between WT and SLP-2 T-K/O T cells, as shown in Fig. 3C (complexes I, III_2, and V) and D (complexes II and IV). Furthermore, 2D BN SDS-PAGE analysis revealed that PHBs and SLP-2 are associated in high-molecular-weight protein complexes, as observed in both first-dimension (Fig. 3A) and second-dimension (Fig. 3C) gels. Taken together, these results show that lack of SLP-2 expression is associated with deficient RCS formation *in vivo*.

Formation of individual respiratory complexes is not affected by SLP-2 deficiency. To determine whether the defect in supercomplex formation in SLP-2-deficient cells was a result of defective formation of individual respiratory complexes, we solubilized mitochondrial membranes with the detergent dodecyl maltoside, which has been shown to disrupt RCS formation while maintaining individual respiratory complex interactions (15). Immunoblotting of membranes from first-dimension BN PAGE gels showed no differences between the levels of individual complex I, II, III, IV, or V in SLP-2 T-K/O T cells and those in WT controls (Fig. 4A). Subsequent immunoblotting for PHB1 and SLP-2 (Fig. 4B and C, respectively) showed that these proteins maintain their migration pattern at high molecular weight when membranes are solubilized with dodecyl maltoside rather than

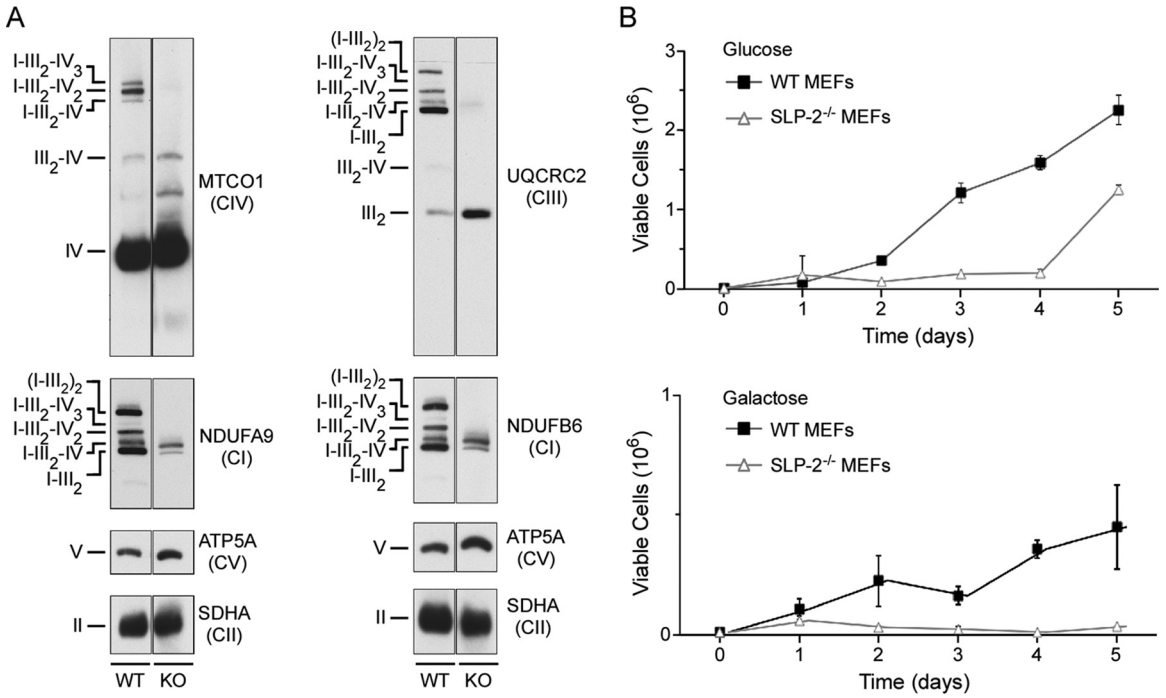

FIG 2 Reduced RCS detection and cell growth in *Slp-2*$^{-/-}$ mutant MEFs. (A) BN PAGE immunoblot analysis of mitochondria isolated from WT and *Slp-2*$^{-/-}$ mutant immortalized fibroblasts. To visualize individual complexes and RCS, membranes were blotted with antibodies directed against complexes IV (MTCO1) and I (NDUFA9) (left side) or complexes III (UQCRC2) and I (NDUFB6) (right side). Membranes were subsequently blotted for complexes II (SDHA) and V (ATP5A). (B) Counts of viable WT and *Slp-2*$^{-/-}$ mutant fibroblasts cultured in 25 mM glucose- or galactose-containing medium were determined every 24 h for 5 days by trypan blue exclusion from an initial seeding of 50,000 cells. Data are the means ± the standard deviations from three independent experiments.

digitonin (Fig. 3A). These results indicated that the defect observed in the formation of RCS in the absence of SLP-2 was not a result of a deficiency in individual respiratory complex formation.

SLP-2 deficiency results in delayed T cell proliferation under conditions of limited glycolysis. We next studied the functional consequences of impaired formation of RCS in SLP-2-deficient T cells. This system provided us with the opportunity to assess the activation and proliferation of WT and SLP-2 T-K/O T cells in response to anti-CD3/CD28 stimulation under conditions of either unlimited or limited glycolysis. First we assessed early activation events by determining the upregulation of CD25 and the downregulation of CD62L by flow cytometry. CD25 was significantly upregulated following activation of WT and SLP-2 T-K/O T cells (Fig. 5A, left side). Such upregulation was significantly decreased in T cells activated under conditions of restricted glycolysis (i.e., galactose-containing medium) or restricted oxidative phosphorylation (i.e., oligomycin-containing medium), yet neither depended upon SLP-2. CD62L expression was decreased under all activation conditions, and this downregulation was also unaffected by SLP-2 deficiency (Fig. 5A, middle). The viability of T cells was unaffected under all activation conditions, except when T cells were restricted in the ability to use both glycolysis and oxidative phosphorylation, under which condition almost all T cells died (Fig. 5A, right side). These results indicated that deficiency of SLP-2 in T cells did not affect early activation events.

Next, we studied the effect of SLP-2 deficiency on T cell cycling. We found that SLP-2-deficient T cells proliferated similarly to WT T cells under conditions of maximal activation with anti-CD3/CD28 and an unlimited supply of glucose (Fig. 5B). However, under conditions of limited glycolysis, SLP-2-deficient T cells displayed a significantly delayed proliferation profile (Fig. 5B). On a population level and after 3 days of stimulation, only 18% of SLP-2-deficient T cells had gone into high cycling, compared to 37% of WT T cells, whereas 47% of SLP-2-deficient T cells remained in low cycling, compared to only 24% of WT T cells (Fig. 5C). By day 3 after stimulation, SLP-2-deficient T cells were, on average, delayed by at least one cycle (Fig. 5D) and this could not be attributed to decreased cell viability (Fig. 5E). Furthermore, we found that SLP-2-deficient T cells cultured under glucose-restricted conditions were delayed in entry into the cell cycle 37 h following stimulation, as determined by the delayed increase in Ki67 expression (Fig. 5F). Nonstimulated cells cultured in glucose and stimulated cells cultured with neither glucose nor galactose exhibited poor viability after 24 h and failed to proliferate after up to 5 days (data not shown).

To examine the cause of the delayed proliferation of SLP-2-deficient T cells, we determined the IL-2 response of these T cells to anti-CD3/CD28 stimulation under conditions of unlimiting and limiting glycolysis. As shown in Fig. 6A, SLP-2-deficient T cells had decreased production of IL-2. Such a defect was apparent both in cultures containing glucose and in cultures containing galactose but not glucose. Furthermore, as we had previously shown, the defective IL-2 response in SLP-2-deficient T cells was a result of a posttranscriptional mechanism as the production of IL-2 mRNA was similar in WT and SLP-2-deficient T cells cultured in glucose-containing (Fig. 6B) or galactose-containing (Fig. 6C) medium. To further elucidate the mechanism responsible for the impairment in IL-2 production, we performed intra-

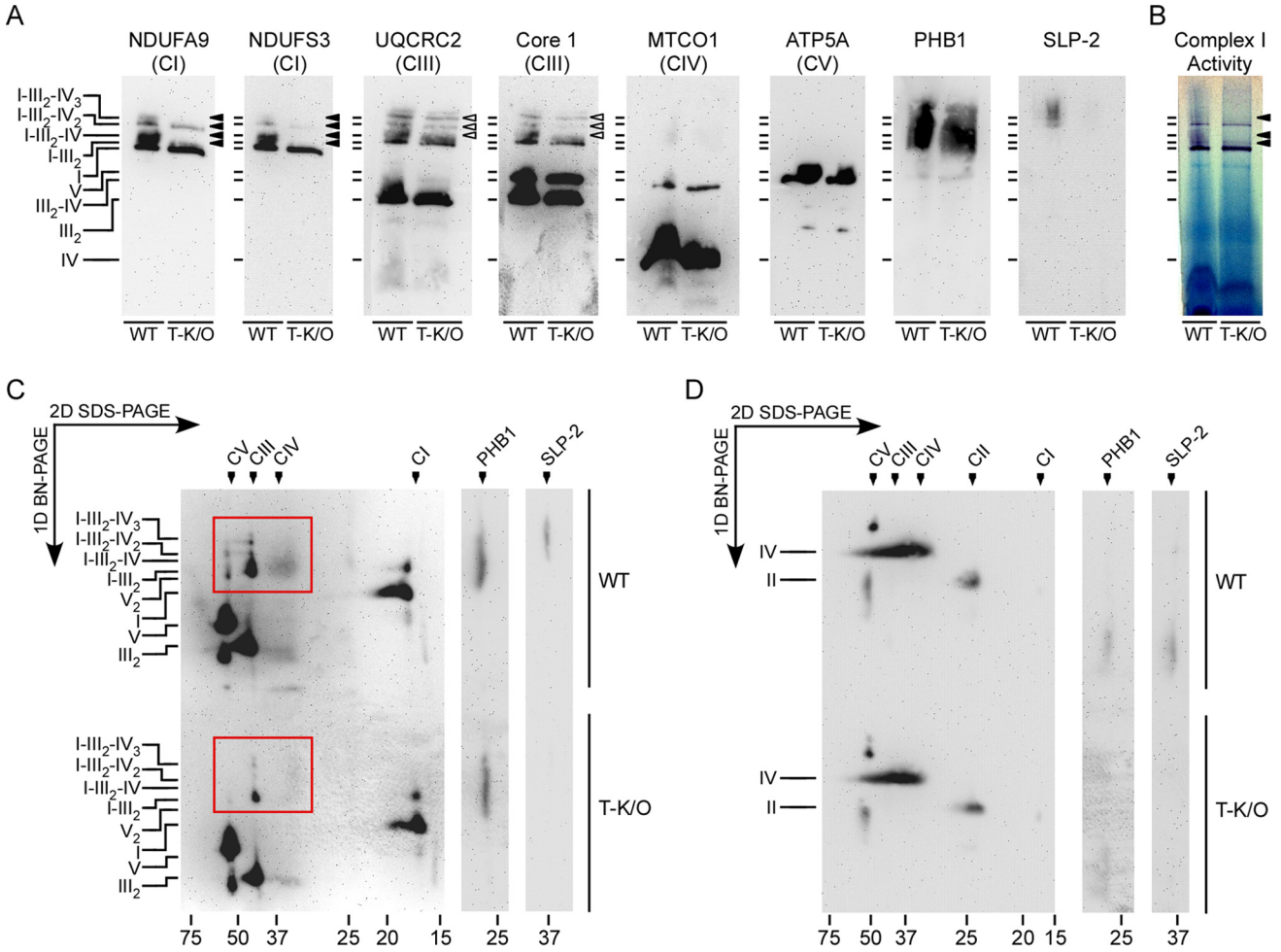

FIG 3 SLP-2-deficient T cells have defective RCS expression. Digitonin-solubilized mitochondrial lysates from WT or SLP-2 T-K/O T cells were separated by BN PAGE under nondenaturing conditions. (A) Membranes of 1D gels were immunoblotted a maximum of two times with antibodies against subunits of each respiratory complex as follows: NDUFA9, NDUFS3; UQCRC2, complex III core 1; MTCO1 (complex IV subunit I); ATP synthase subunit alpha (ATP5A); PHB1; and SLP-2. The stoichiometries of each RCS band are indicated, and arrows point to the most apparent defects. (B) In-gel complex I activity was determined on a 1D BN PAGE gel. Purple color indicates areas of complex I activity. Arrowheads indicate RCS containing decreased levels of complex I subunits (A) or activity (B; filled) or complex III subunits (A; open) when *Slp-2* is deleted. First-dimension gel slices were cut and loaded onto second-dimension denaturing gels to compare high-molecular-weight (C) and low-molecular-weight (D) complexes. Membranes were immunoblotted with antibodies against respiratory chain subunits (CI, complex I subunit NDUFB8; CII, complex II subunit 30 kDa; CIII, complex III subunit core 2; CIV, complex IV subunit I; CV, ATP synthase subunit alpha) and then PHB1 and SLP-2. Red boxes indicate RCS containing decreased levels of complex I, III, IV, and V subunits. Data are representative of three (A, C, D) or two (B) independent experiments.

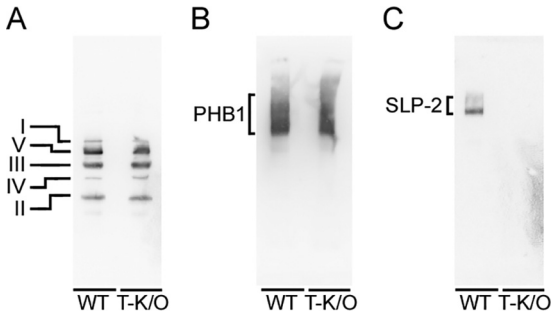

FIG 4 Formation of individual respiratory chain complexes is not altered by *Slp-2* deletion. Dodecyl maltoside-solubilized mitochondrial lysates from WT or SLP-2 T-K/O T cells were separated by BN PAGE under nondenaturing conditions. Membranes were immunoblotted with a cocktail of antibodies against respiratory chain subunits (I, complex I subunit NDUFB8; II, complex II subunit 30 kDa; III, complex III subunit core 2; IV, complex IV subunit I; V, ATP synthase subunit alpha) (A) and then PHB1 (B) and SLP-2 (C).

cellular IL-2 staining of anti-CD3/CD28-stimulated WT and SLP-2 T-K/O T cells treated with brefeldin A at the time of stimulation to prevent cytokine secretion. We found that the percentage of IL-2$^+$ SLP-2 T-K/O T cells was reduced relative to that of WT T cells when cultured in glucose-containing (16.2 versus 22.5%) or galactose-containing (18.1 versus 28.3%) medium. These data indicate that the posttranscriptional impairment of IL-2 production in SLP-2 T-K/O T cells is likely due to a defect in protein translation and not secretion. Although the IL-2 levels were decreased, we found no difference in IκB phosphorylation (Fig. 6D) or mitochondrial calcium release (Fig. 6E) following stimulation, suggesting normal T cell signaling. To determine whether the lower IL-2 levels were responsible for the delayed proliferation of glucose-restricted SLP-2-deficient T cells, we supplemented the cultures with 50 ng/ml mrIL-2 at the time of stimulation. However, this did not restore the delay in proliferation of

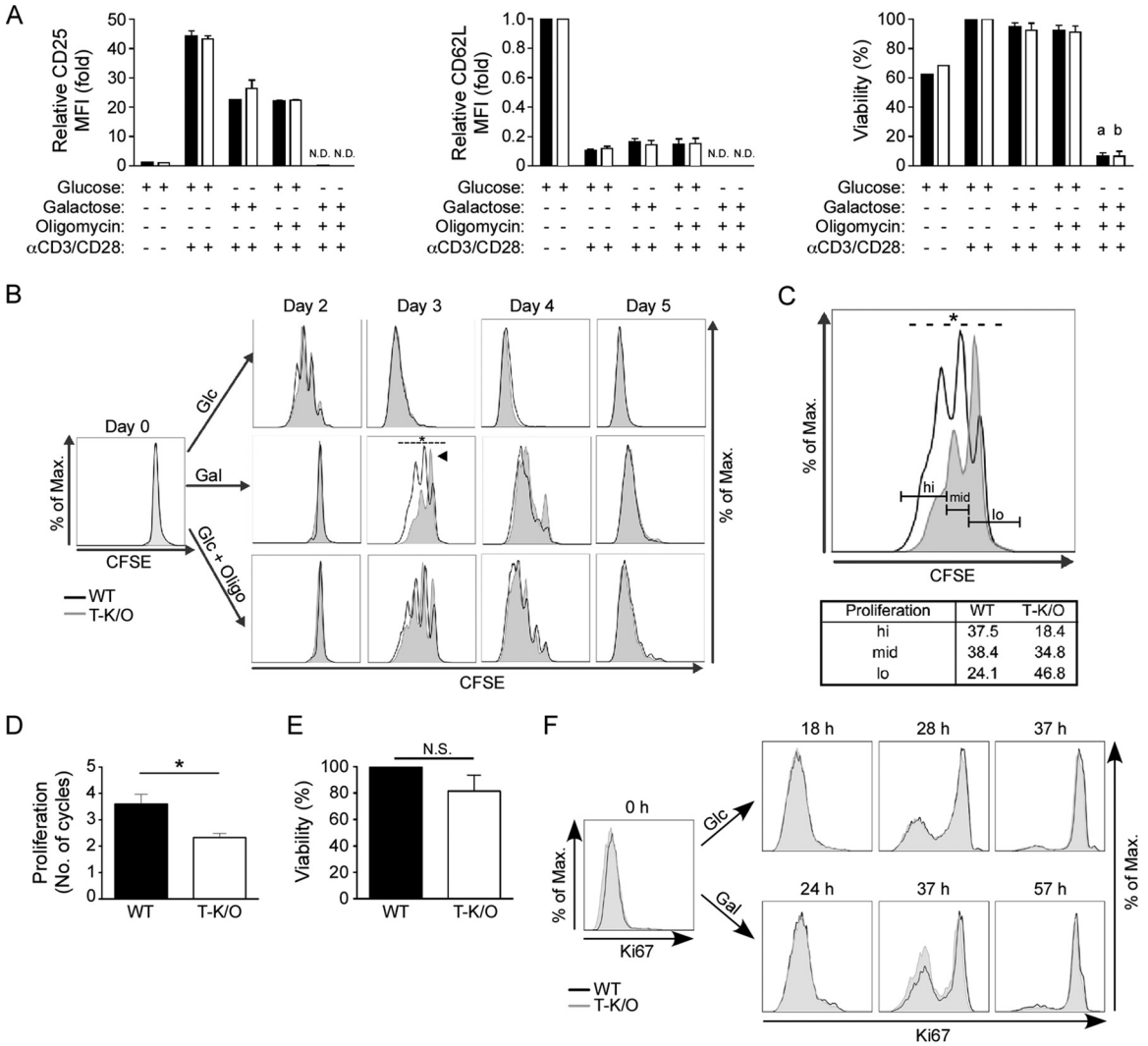

FIG 5 Deletion of *Slp-2* results in delayed T cell proliferation when glycolysis is restricted. WT (black bars) and SLP-2 T-K/O T (white bars) cells were resting or stimulated in glucose (Glc)- or galactose (Gal)-containing medium with or without oligomycin (Oligo) for the times indicated. (A) Expression of CD25 and CD62L was measured after 0 and 24 h by flow cytometry ($n = 3$), and data are represented as fold changes in the geometric mean fluorescence intensity (MFI) relative to that of resting T cells at 0 h. Viability was concurrently measured and was normalized to the glucose-only condition. N.D., not detected. a, $P < 0.001$ relative to WT T cells in glucose-containing medium; b, $P < 0.001$ relative to SLP-2 T-K/O T cells in glucose-containing medium. (B) T cell proliferation was assessed by measurement of CFSE dilution on days 0, 2, 3, 4, and 5 poststimulation by flow cytometry. Plots depict representative WT and SLP-2 T-K/O T cell distributions ($n = 3$). (C) CFSE distribution of WT and SLP-2 T-K/O T cells on day 3 of growth in galactose-containing medium is expanded from panel B, and three proliferative subsets (hi, mid, and lo) are indicated. (D) The number of proliferation cycles of T cells stimulated in galactose-containing medium was calculated by taking the $\log_{1/2}$ of the relative CFSE geometric MFI normalized to day 0. (E) Cell viability of CFSE-stained cells was measured at day 3 by flow cytometry. (F) Stimulated cells cultured in glucose- or galactose-containing medium were analyzed for cellular Ki67 expression by flow cytometry. Data are reported as the mean ± the standard error of the mean. *, $P < 0.05$. N.S., not significant.

glucose-restricted SLP-2-deficient T cells (Fig. 6F), indicating an alternate mechanism. Altogether, these results documented a functional defect associated with the impaired formation of RCS in the absence of SLP-2.

DISCUSSION

The molecular machinery that supports the optimal assembly and function of respiratory complexes in the mitochondrial inner membrane is not fully defined. Recent evidence suggests that different proteins may be involved in the assembly of individual components of the respiratory chain into RCS, i.e., assemblies of respiratory chain complexes with defined stoichiometries. In the context of this model, our findings identify SLP-2 as a critical player in the formation of these RCS, specifically, $(\text{I-III}_2)_{1\text{-}2}$, $\text{I-III}_2\text{-IV}_3$, $\text{I-III}_2\text{-IV}_2$, $\text{I-III}_2\text{-IV}$, I-III_2, and $\text{III}_2\text{-IV}$ arrangements, and potentially complex V-containing dimers and multimers. The precise mechanism by which SLP-2 affects RCS formation, whether it is important primarily for RCS assembly or stability or rather for regulating the expression of individual respiratory complex subunits, is unknown and is beyond the scope of this study. However, our data indicate that the mechanism responsible for defective RCS formation in the absence of SLP-2 does not relate to the improper formation of individual respiratory complexes. Using T cells from a genetically engineered mouse strain in which the *Slp-2*

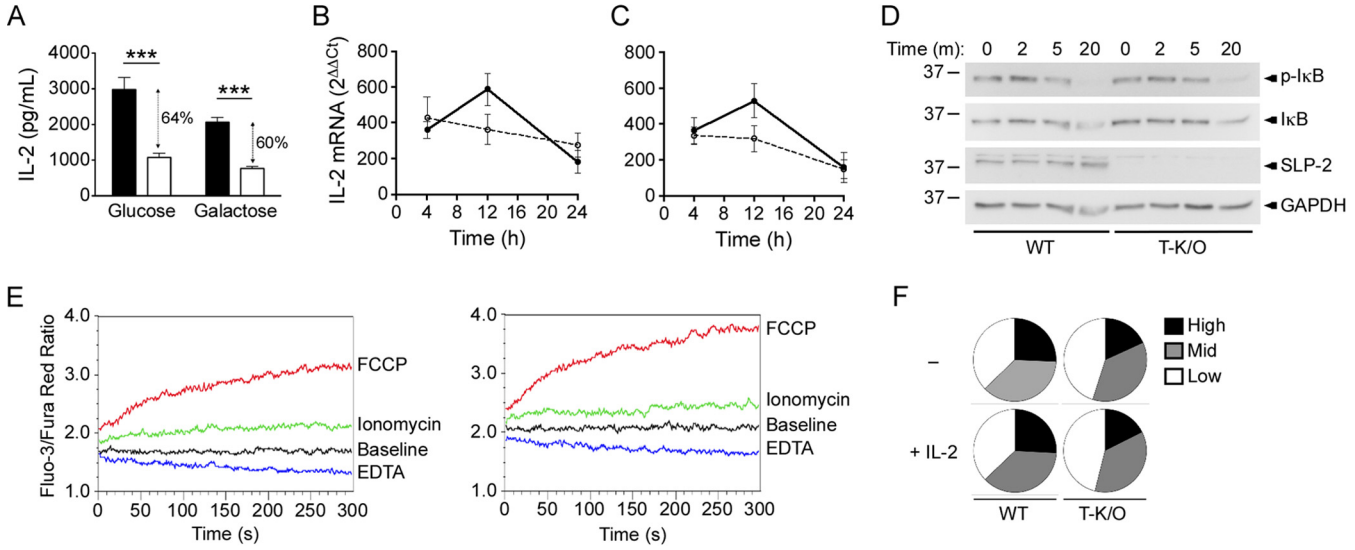

FIG 6 Deletion of *Slp-2* results in defective posttranscriptional IL-2 production when glycolysis is restricted. WT and SLP-2 T-K/O T cells were stimulated in glucose- or galactose-containing medium for the times indicated. (A) IL-2 protein levels were measured in supernatants by ELISA at 24 h following stimulation of WT (black bars) or SLP-2 T-K/O T (white bars) cells in glucose- or galactose-containing medium. IL-2 mRNA levels were assessed by quantitative reverse transcriptase PCR at 4, 12, and 24 h poststimulation in glucose (B)- or galactose (C)-containing medium (WT, closed circles; SLP-2 T-K/O, open circles). (D) WT or SLP-2 T-K/O T cells were stimulated with anti-CD3/CD28 antibody-coated beads for the times indicated, and whole-cell lysates were blotted with anti-phospho-IκB, anti-IκB, anti-SLP-2, and anti-GAPDH antibodies. The values on the left axis are molecular masses in kilodaltons. (E) Calcium release was determined by flow cytometry in WT (left side) or SLP-2 T-K/O (right side) T cells by measuring the Fluo-3-AM/Fura Red ratio. Samples were analyzed for baseline fluorescence and then analyzed immediately following the addition of 2 μg/ml ionomycin, 50 nM FCCP (positive control), or 5 mM EDTA (negative control). (F) Proliferation profiles of stimulated CFSE-stained cells supplemented with or without mrIL-2 (50 ng/ml) at $t = 0$ h. Pie charts indicate the percentages of cells in low, medium, and high proliferative states after 72 h. Data are reported as the mean ± the standard error of the mean. ***, $P < 0.001$.

gene is specifically deleted in T cell progenitors, we have shown here that the defect in RCS formation is linked with an impaired respiratory profile, more apparent under conditions of limited glycolysis, and this translates into a defective functional T cell response.

There is evidence to suggest that the lipid composition of the mitochondrial inner membrane is key for proper RCS formation, particularly since the interactions between complexes occur within the lipid bilayer of the membrane while the matrix portions do not strongly interact (14). The mitochondrial signature phospholipid cardiolipin is a critical component of this environment and has been shown to be essential for proper RCS formation (8, 14, 22), with defective cardiolipin remodeling and RCS instability associated with Barth syndrome (7, 20). We have previously shown that SLP-2 binds cardiolipin and interacts with PHB1 and -2, and that in SLP-2-deficient T cells, the levels of cardiolipin and PHBs in mitochondrial detergent-insoluble membranes are significantly decreased (5, 6). As a consequence, a deficiency in SLP-2 expression would impair the proper compartmentalization of the mitochondrial membrane and result in defective RCS formation. This would be consistent with the evidence that SLP-2 can dimerize (1) and may form homooligomeric complexes similar to PHBs (45). Indeed, SLP-2 was found to migrate in a high-molecular-weight complex by BN PAGE in rat liver, potentially as a homooligomeric complex (42), and a recent report has claimed that a plant homologue of *Slp-2* in *Arabidopsis thaliana* may also be linked to RCS organization in plants (46). These reports corroborate our findings and, together with our data showing impaired RCS formation in both *Slp-2*$^{-/-}$ MEFs and SLP-2-deficient T cells, point to a critical role for SLP-2 in RCS formation, one that is potentially conserved across different tissues and species.

The abnormal compartmentalization of cardiolipin in the absence of SLP-2 may explain the defective RCS formation, particularly of $(\text{I-III}_2)_{1\text{-}2}$ and $\text{I-III}_2\text{-IV}_{1\text{-}3}$ arrangements. The formation of cardiolipin-enriched membrane microdomains facilitated by SLP-2 (5, 6) may provide a platform for optimal RCS assembly and/or stability in the inner membrane of the mitochondria. Formation of these microdomains likely involves PHBs in addition to SLP-2, and PHBs have been previously proposed to be involved in the assembly of respiratory complexes (35). PHBs comigrate with RCS by 2D BN SDS-PAGE in this study and in reference 15, while SLP-2 also migrated with RCS, though at a slightly lower rate than PHBs. The interaction between SLP-2 and PHBs (5, 6, 44) may have structural and functional implications in the regulation of mitochondrial function (47), though PHB oligomerization is not affected by *Slp-2* deletion in our model. As we previously reported, our data show that the levels of PHBs present in the detergent (i.e., Triton X-100, digitonin, or dodecyl maltoside)-soluble fraction of mitochondrial lysates in the absence of SLP-2 are not different from control levels (5). Furthermore, SLP-2 does not seem to interact directly with RCS because experiments with plant mitochondria using complex I mutants lacking proper RCS associations showed that the migration pattern of a plant *Slp-2* homolog is largely unchanged (46). It has also recently been reported that the *Cox7a2l* gene in several strains of mice, including C57BL/6J, carries a mutation that prevents the formation of complex IV-containing RCS. The mouse strains used in this study have a C57BL/6N Tac background, and our data demonstrate that these mice retain the ability to form complex IV-containing RCS.

The defective formation of RCS was associated with an impaired respiratory profile. This profile is characterized by increased uncoupled respiration, decreased mitochondrial mem-

brane potential, and an increased reliance on glycolysis. In addition, we observed a slight but significant increase in ROS produced upon stimulation of SLP-2-deficient T cells. ROS are produced by the respiratory chain under normal circumstances (48), and defective RCS formation, particularly of I-III-containing RCS, leads to increased ROS production (14). This supports our findings of defective $(I\text{-}III_2)_{1\text{-}2}$ and $I\text{-}III_2\text{-}IV_{1\text{-}3}$ RCS formation in the absence of SLP-2.

It has recently been reported that either glycolysis or oxidative phosphorylation alone is sufficient to sustain normal T cell proliferation in response to activation (49). SLP-2 plays a role in T cell activation (50), and its deficiency is associated with impaired T cell responses (5). We show here that proliferation of SLP-2 T-K/O T cells is not significantly affected compared to that of WT T cells when oxidative phosphorylation is restricted if glycolysis is not limiting but is significantly delayed when glycolysis is restricted. Furthermore, this delay in proliferation is due in part to delayed entry into the cell cycle. These findings would be expected in light of the bioenergetic profile of these T cells and suggest that the metabolic output of the respiratory chain in SLP-2 T-K/O T cells is insufficient to meet the requirements of optimal T cell proliferation. Such a defect may be secondary to impaired RCS assembly and/or stability and results in delayed proliferation. However, this delayed cycling cannot be rescued by restoration of IL-2 levels, indicating the involvement of other factors.

Chang and colleagues have recently reported that the expression of several cytokines, including IL-2 and gamma interferon (IFN-γ), is decreased when glycolysis is restricted (49). This decrease in cytokine expression is mediated by a posttranscriptional mechanism involving an increased ability for GAPDH to bind to AU-rich elements within the 3′ untranslated region of these respective mRNAs, effectively reducing their translation in response to decreased glycolysis (49). We had already shown that SLP-2-deficient T cells have a posttranscriptional defect in IL-2 production in response to stimulation through the antigen receptor (5). However, contrary to the observation by Chang et al. with limited glycolysis in WT cells, the defect observed in SLP-2-deficient T cells is selective for IL-2 and does not occur for other cytokines such as IFN-γ or IL-17. Furthermore, the posttranscriptional IL-2 defect in SLP-2-deficient T cells is present to the same extent under conditions of limiting or unlimiting glycolysis and is likely a result of impaired protein translation and not secretion. Altogether, these results suggest that the mechanism responsible for the posttranscriptional defect in IL-2 production in SLP-2 T-K/O T cells is independent of GAPDH and may involve a novel pathway linked to impaired mitochondrial respiration.

In summary, our data show that SLP-2 is required for optimal RCS formation in the mitochondrial inner membrane. In the absence of SLP-2, there is significant loss of $(I\text{-}III_2)_{1\text{-}2}$ and $I\text{-}III_2\text{-}IV_{1\text{-}3}$ RCS, which may be due to a defect in the assembly or a lack of stability of these supercomplexes. More importantly, abnormal RCS expression correlates with impaired mitochondrial respiration and results in decreased effector cell function. Further studies are required to determine the mechanism whereby SLP-2 functions to allow optimal RCS formation: whether it is a direct function of SLP-2 or rather if it is indirect, perhaps through the generation of specialized cardiolipin-enriched microdomains in the mitochondrial inner membrane. Together, these findings provide evidence that RCS are a relevant functional entity and identify SLP-2 as a key player in the assembly and/or stability of these supercomplexes.

ACKNOWLEDGMENTS

We thank Julie St-Pierre, Heidi McBride, and Eric Shoubridge (McGill University) for helpful comments regarding bioenergetics and BN gel electrophoresis; Russell Jones (McGill University) for access to the Seahorse XF analyzer; and members of the Madrenas laboratory for comments and criticisms.

This work was funded by grants from the Canadian Institutes of Health Research to J.M. and the European Research Council to T.L. T.W. holds an HFSP long-term fellowship. J.M. holds a Tier I Canada Research Chair in Human Immunology.

REFERENCES

1. **Christie DA, Kirchhof MG, Vardhana S, Dustin ML, Madrenas J.** 2012. Mitochondrial and plasma membrane pools of stomatin-like protein 2 coalesce at the immunological synapse during T cell activation. PLoS One **7:**e37144. http://dx.doi.org/10.1371/journal.pone.0037144.
2. **Da Cruz S, Xenarios I, Langridge J, Vilbois F, Parone PA, Martinou JC.** 2003. Proteomic analysis of the mouse liver mitochondrial inner membrane. J Biol Chem **278:**41566–41571. http://dx.doi.org/10.1074/jbc.M304940200.
3. **Taylor SW, Fahy E, Zhang B, Glenn GM, Warnock DE, Wiley S, Murphy AN, Gaucher SP, Capaldi RA, Gibson BW, Ghosh SS.** 2003. Characterization of the human heart mitochondrial proteome. Nat Biotechnol **21:**281–286. http://dx.doi.org/10.1038/nbt793.
4. **Green JB, Young JP.** 2008. Slipins: ancient origin, duplication and diversification of the stomatin protein family. BMC Evol Biol **8:**44. http://dx.doi.org/10.1186/1471-2148-8-44.
5. **Christie DA, Mitsopoulos P, Blagih J, Dunn SD, St-Pierre J, Jones RG, Hatch GM, Madrenas J.** 2012. Stomatin-like protein 2 deficiency in T cells is associated with altered mitochondrial respiration and defective $CD4^+$ T cell responses. J Immunol **189:**4349–4360. http://dx.doi.org/10.4049/jimmunol.1103829.
6. **Christie DA, Lemke CD, Elias IM, Chau LA, Kirchhof MG, Li B, Ball EH, Dunn SD, Hatch GM, Madrenas J.** 2011. Stomatin-like protein 2 binds cardiolipin and regulates mitochondrial biogenesis and function. Mol Cell Biol **31:**3845–3856. http://dx.doi.org/10.1128/MCB.05393-11.
7. **Acin-Pérez R, Enriquez JA.** 2014. The function of the respiratory supercomplexes: the plasticity model. Biochim Biophys Acta **1837:**444–450. http://dx.doi.org/10.1016/j.bbabio.2013.12.009.
8. **Lenaz G, Genova ML.** 2012. Supramolecular organisation of the mitochondrial respiratory chain: a new challenge for the mechanism and control of oxidative phosphorylation. Adv Exp Med Biol **748:**107–144. http://dx.doi.org/10.1007/978-1-4614-3573-0_5.
9. **Schägger H, von Jagow G.** 1991. Blue native electrophoresis for isolation of membrane protein complexes in enzymatically active form. Anal Biochem **199:**223–231. http://dx.doi.org/10.1016/0003-2697(91)90094-A.
10. **Schägger H, Pfeiffer K.** 2000. Supercomplexes in the respiratory chains of yeast and mammalian mitochondria. EMBO J **19:**1777–1783. http://dx.doi.org/10.1093/emboj/19.8.1777.
11. **Dudkina NV, Kudryashev M, Stahlberg H, Boekema EJ.** 2011. Interaction of complexes I, III, and IV within the bovine respirasome by single particle cryoelectron tomography. Proc Natl Acad Sci U S A **108:**15196–15200. http://dx.doi.org/10.1073/pnas.1107819108.
12. **Althoff T, Mills DJ, Popot JL, Kuhlbrandt W.** 2011. Arrangement of electron transport chain components in bovine mitochondrial supercomplex I1III2IV1. EMBO J **30:**4652–4664. http://dx.doi.org/10.1038/emboj.2011.324.
13. **Seelert H, Dencher NA.** 2011. ATP synthase superassemblies in animals and plants: two or more are better. Biochim Biophys Acta **1807:**1185–1197. http://dx.doi.org/10.1016/j.bbabio.2011.05.023.
14. **Lenaz G, Baracca A, Barbero G, Bergamini C, Dalmonte ME, Del Sole M, Faccioli M, Falasca A, Fato R, Genova ML, Sgarbi G, Solaini G.** 2010. Mitochondrial respiratory chain super-complex I-III in physiology and pathology. Biochim Biophys Acta **1797:**633–640. http://dx.doi.org/10.1016/j.bbabio.2010.01.025.
15. **Acin-Pérez R, Fernandez-Silva P, Peleato ML, Pérez-Martos A, Enriquez JA.** 2008. Respiratory active mitochondrial supercomplexes. Mol Cell **32:**529–539. http://dx.doi.org/10.1016/j.molcel.2008.10.021.
16. **Lapuente-Brun E, Moreno-Loshuertos R, Acin-Pérez R, Latorre-Pellicer**

A, Colas C, Balsa E, Perales-Clemente E, Quiros PM, Calvo E, Rodriguez-Hernandez MA, Navas P, Cruz R, Carracedo A, Lopez-Otin C, Pérez-Martos A, Fernandez-Silva P, Fernandez-Vizarra E, Enriquez JA. 2013. Supercomplex assembly determines electron flux in the mitochondrial electron transport chain. Science **340:**1567–1570. http://dx.doi.org/10.1126/science.1230381.

17. **Vartak R, Porras CA, Bai Y.** 2013. Respiratory supercomplexes: structure, function and assembly. Protein Cell **4:**582–590. http://dx.doi.org/10.1007/s13238-013-3032-y.
18. **Schägger H, de Coo R, Bauer MF, Hofmann S, Godinot C, Brandt U.** 2004. Significance of respirasomes for the assembly/stability of human respiratory chain complex I. J Biol Chem **279:**36349–36353. http://dx.doi.org/10.1074/jbc.M404033200.
19. **Acin-Pérez R, Bayona-Bafaluy MP, Fernandez-Silva P, Moreno-Loshuertos R, Pérez-Martos A, Bruno C, Moraes CT, Enriquez JA.** 2004. Respiratory complex III is required to maintain complex I in mammalian mitochondria. Mol Cell **13:**805–815. http://dx.doi.org/10.1016/S1097-2765(04)00124-8.
20. **McKenzie M, Lazarou M, Thorburn DR, Ryan MT.** 2006. Mitochondrial respiratory chain supercomplexes are destabilized in Barth syndrome patients. J Mol Biol **361:**462–469. http://dx.doi.org/10.1016/j.jmb.2006.06.057.
21. **Potting C, Tatsuta T, Konig T, Haag M, Wai T, Aaltonen MJ, Langer T.** 2013. TRIAP1/PRELI complexes prevent apoptosis by mediating intramitochondrial transport of phosphatidic acid. Cell Metab **18:**287–295. http://dx.doi.org/10.1016/j.cmet.2013.07.008.
22. **Pfeiffer K, Gohil V, Stuart RA, Hunte C, Brandt U, Greenberg ML, Schägger H.** 2003. Cardiolipin stabilizes respiratory chain supercomplexes. J Biol Chem **278:**52873–52880. http://dx.doi.org/10.1074/jbc.M308366200.
23. **Arnarez C, Mazat JP, Elezgaray J, Marrink SJ, Periole X.** 2013. Evidence for cardiolipin binding sites on the membrane-exposed surface of the cytochrome bc1. J Am Chem Soc **135:**3112–3120. http://dx.doi.org/10.1021/ja310577u.
24. **Arnarez C, Marrink SJ, Periole X.** 2013. Identification of cardiolipin binding sites on cytochrome *c* oxidase at the entrance of proton channels. Sci Rep **3:**1263. http://dx.doi.org/10.1038/srep01263.
25. **Eble KS, Coleman WB, Hantgan RR, Cunningham CC.** 1990. Tightly associated cardiolipin in the bovine heart mitochondrial ATP synthase as analyzed by 31P nuclear magnetic resonance spectroscopy. J Biol Chem **265:**19434–19440.
26. **Fry M, Green DE.** 1981. Cardiolipin requirement for electron transfer in complex I and III of the mitochondrial respiratory chain. J Biol Chem **256:**1874–1880.
27. **Fry M, Green DE.** 1980. Cardiolipin requirement by cytochrome oxidase and the catalytic role of phospholipid. Biochem Biophys Res Commun **93:**1238–1246. http://dx.doi.org/10.1016/0006-291X(80)90622-1.
28. **Jiang F, Ryan MT, Schlame M, Zhao M, Gu Z, Klingenberg M, Pfanner N, Greenberg ML.** 2000. Absence of cardiolipin in the crd1 null mutant results in decreased mitochondrial membrane potential and reduced mitochondrial function. J Biol Chem **275:**22387–22394. http://dx.doi.org/10.1074/jbc.M909868199.
29. **Chen YC, Taylor EB, Dephoure N, Heo JM, Tonhato A, Papandreou I, Nath N, Denko NC, Gygi SP, Rutter J.** 2012. Identification of a protein mediating respiratory supercomplex stability. Cell Metab **15:**348–360. http://dx.doi.org/10.1016/j.cmet.2012.02.006.
30. **Vukotic M, Oeljeklaus S, Wiese S, Vogtle FN, Meisinger C, Meyer HE, Zieseniss A, Katschinski DM, Jans DC, Jakobs S, Warscheid B, Rehling P, Deckers M.** 2012. Rcf1 mediates cytochrome oxidase assembly and respirasome formation, revealing heterogeneity of the enzyme complex. Cell Metab **15:**336–347. http://dx.doi.org/10.1016/j.cmet.2012.01.016.
31. **Strogolova V, Furness A, Robb-McGrath M, Garlich J, Stuart RA.** 2012. Rcf1 and Rcf2, members of the hypoxia-induced gene 1 protein family, are critical components of the mitochondrial cytochrome bc1-cytochrome *c* oxidase supercomplex. Mol Cell Biol **32:**1363–1373. http://dx.doi.org/10.1128/MCB.06369-11.
32. **Ikeda K, Shiba S, Horie-Inoue K, Shimokata K, Inoue S.** 2013. A stabilizing factor for mitochondrial respiratory supercomplex assembly regulates energy metabolism in muscle. Nat Commun **4:**2147. http://dx.doi.org/10.1038/ncomms3147.
33. **Merkwirth C, Dargazanli S, Tatsuta T, Geimer S, Lower B, Wunderlich FT, von Kleist-Retzow JC, Waisman A, Westermann B, Langer T.** 2008. Prohibitins control cell proliferation and apoptosis by regulating OPA1-dependent cristae morphogenesis in mitochondria. Genes Dev **22:**476–488. http://dx.doi.org/10.1101/gad.460708.
34. **Anand R, Wai T, Baker MJ, Kladt N, Schauss AC, Rugarli E, Langer T.** 2014. The i-AAA protease YME1L and OMA1 cleave OPA1 to balance mitochondrial fusion and fission. J Cell Biol **204:**919–929. http://dx.doi.org/10.1083/jcb.201308006.
35. **Nijtmans LG, Henderson NS, Holt IJ.** 2002. Blue native electrophoresis to study mitochondrial and other protein complexes. Methods **26:**327–334. http://dx.doi.org/10.1016/S1046-2023(02)00038-5.
36. **Mitsopoulos P, Madrenas J.** 2013. Identification of multimolecular complexes and supercomplexes in compartment-selective membrane microdomains. Methods Cell Biol **117:**411–431. http://dx.doi.org/10.1016/B978-0-12-408143-7.00022-0.
37. **Sasarman F, Antonicka H, Shoubridge EA.** 2008. The A3243G tRNALeu(UUR) MELAS mutation causes amino acid misincorporation and a combined respiratory chain assembly defect partially suppressed by overexpression of EFTu and EFG2. Hum Mol Genet **17:**3697–3707. http://dx.doi.org/10.1093/hmg/ddn265.
38. **Jung C, Higgins CM, Xu Z.** 2000. Measuring the quantity and activity of mitochondrial electron transport chain complexes in tissues of central nervous system using blue native polyacrylamide gel electrophoresis. Anal Biochem **286:**214–223. http://dx.doi.org/10.1006/abio.2000.4813.
39. **Brand MD, Nicholls DG.** 2011. Assessing mitochondrial dysfunction in cells. Biochem J **435:**297–312. http://dx.doi.org/10.1042/BJ20110162.
40. **Bustamante E, Pedersen PL.** 1977. High aerobic glycolysis of rat hepatoma cells in culture: role of mitochondrial hexokinase. Proc Natl Acad Sci U S A **74:**3735–3739. http://dx.doi.org/10.1073/pnas.74.9.3735.
41. **Boudina S, Sena S, Theobald H, Sheng X, Wright JJ, Hu XX, Aziz S, Johnson JI, Bugger H, Zaha VG, Abel ED.** 2007. Mitochondrial energetics in the heart in obesity-related diabetes: direct evidence for increased uncoupled respiration and activation of uncoupling proteins. Diabetes **56:**2457–2466. http://dx.doi.org/10.2337/db07-0481.
42. **Reifschneider NH, Goto S, Nakamoto H, Takahashi R, Sugawa M, Dencher NA, Krause F.** 2006. Defining the mitochondrial proteomes from five rat organs in a physiologically significant context using 2D blue native/SDS-PAGE. J Proteome Res **5:**1117–1132. http://dx.doi.org/10.1021/pr0504440.
43. **Buck KJ, Walter NA, Denmark DL.** 2014. Genetic variability of respiratory complex abundance, organization and activity in mouse brain. Genes Brain Behav **13:**135–143. http://dx.doi.org/10.1111/gbb.12101.
44. **Da Cruz S, Parone PA, Gonzalo P, Bienvenut WV, Tondera D, Jourdain A, Quadroni M, Martinou JC.** 2008. SLP-2 interacts with prohibitins in the mitochondrial inner membrane and contributes to their stability. Biochim Biophys Acta **1783:**904–911. http://dx.doi.org/10.1016/j.bbamcr.2008.02.006.
45. **Tatsuta T, Model K, Langer T.** 2005. Formation of membrane-bound ring complexes by prohibitins in mitochondria. Mol Biol Cell **16:**248–259. http://dx.doi.org/10.1091/mbc.E04-09-0807.
46. **Gehl B, Lee CP, Bota P, Blatt MR, Sweetlove LJ.** 2014. An Arabidopsis stomatin-like protein affects mitochondrial respiratory supercomplex organization. Plant Physiol **164:**1389–1400. http://dx.doi.org/10.1104/pp.113.230383.
47. **Osman C, Voelker DR, Langer T.** 2011. Making heads or tails of phospholipids in mitochondria. J Cell Biol **192:**7–16. http://dx.doi.org/10.1083/jcb.201006159.
48. **Murphy MP.** 2009. How mitochondria produce reactive oxygen species. Biochem J **417:**1–13. http://dx.doi.org/10.1042/BJ20081386.
49. **Chang CH, Curtis JD, Maggi LB, Jr, Faubert B, Villarino AV, O'Sullivan D, Huang SC, van der Windt GJ, Blagih J, Qiu J, Weber JD, Pearce EJ, Jones RG, Pearce EL.** 2013. Posttranscriptional control of T cell effector function by aerobic glycolysis. Cell **153:**1239–1251. http://dx.doi.org/10.1016/j.cell.2013.05.016.
50. **Kirchhof MG, Chau LA, Lemke CD, Vardhana S, Darlington PJ, Marquez ME, Taylor R, Rizkalla K, Blanca I, Dustin ML, Madrenas J.** 2008. Modulation of T cell activation by stomatin-like protein 2. J Immunol **181:**1927–1936. http://dx.doi.org/10.4049/jimmunol.181.3.1927.